

Optimisation of ex-situ annealing process for epitaxial silicon emitters via Hot Wire CVD

Edris Khorani^{1*}, Tudor Scheul¹, Antulio Tarazona², Tasmiat Rahman¹, Stuart A Boden¹

¹Electronics and Computer Science, University of Southampton, Southampton, SO17 1BJ, UK

²Optoelectronics Research Centre, University of Southampton, Southampton, SO17 1BJ, UK

*Corresponding Author: ek9g13@soton.ac.uk

Abstract

A refined Hot Wire Chemical Vapour Deposition (HWCVD) process for fabricating boron doped silicon emitters using a shortened anneal time and temperature is presented. We are able to crystallise our grown films with a post-deposition annealing treatment of 2 minutes at 800°C, a significant improvement from previous work using several hours at 1000°C. Direct implications of higher annealing temperatures on the film quality is discussed. In addition, the potential for in-situ annealing using a higher deposition temperature is presented, with future works aiming to find and apply the optimum deposition temperature for epitaxial silicon with HWCVD.

Introduction

Interdigitated back-contact (IBC) silicon solar cells are amongst the highest performing single junction solar cells with current records in power conversion efficiency (PCE) exceeding 26% [1]. The absence of front contacts enables the minimization of optical losses in the IBC design, leading to an increase in current density of up to 8% [2]. Moreover, this allows the development of further novel applications such as tandem configurations and more aesthetically pleasing designs using the IBC solar cell.

Despite these advantageous traits, the production cost of diffused junction IBC solar cells remains an issue and the complications in fabrication hinder wide-scale adoption of the design [3]. Thermal diffusion is generally used for both the emitter and back-surface field formation in typical IBC designs [1, 2, 4]. With the potential to achieve shorter deposition times and more uniform doping profiles [5], silicon epitaxy via chemical vapour deposition offers the opportunity to revolutionise current commercial silicon emitter fabrication processes. Our interest

lies on developing a cost-effective and scalable process to eradicate such hindrances by developing an epitaxial Hotwire Chemical Vapour Deposition (HWCVD) process for boron-doped emitter formation. HWCVD has been successfully used to epitaxially grow doped silicon films up to 40 µm thick, with some complete IBC cells utilizing this type of emitter achieving J_{sc} of up to 41 mA/cm² and PCE's exceeding 22% [3, 6, 7].

In this paper, we propose a refined HWCVD process for growing epitaxial silicon, based on previous works [8] which required a post-annealing treatment of between 1-4 hours at 1000°C. The effect of reducing the post-deposition annealing temperature and duration using a rapid thermal anneal (RTA) process is studied, working towards completely eradicating this step in the fabrication process of IBC solar cells via in-situ annealing. This can be done by depositing at a higher temperature within the HWCVD chamber, using a higher number of filaments in the centre region within the chamber. Morphological studies of these films are presented with direct implications of these results on IBC solar cell design.

Doped Silicon Film Fabrication

The wafers used for this experiment were float-zone (FZ) double-side polished, <100>, 280 µm thick and 4" in diameter. The samples were cleaned in fuming HNO₃ solution followed by a native oxide etch in 7:1 buffered HF solution. These were then transferred to the HWCVD tool for the two types of deposition of interest: (i) normal filament configuration (NFC) and (ii) altered filament configuration (AFC) for a higher deposition temperature. An illustration of the NFC and AFC is shown in Figure 1(a) and (b) respectively.

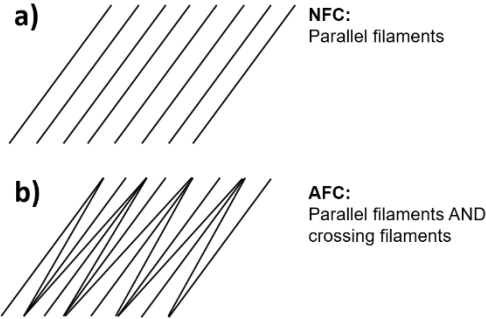


Figure 1: Illustration of filament configuration in (a) NFC and (b) AFC.

The process recipe for depositing the double-sided boron-doped (p-type) emitter film was kept constant for both samples and is based on previous work [5]. This consisted of a 1 minute H_2 chamber conditioning step, followed 23 minutes of SiH_4/B_2H_6 at a 10/10 sccm gas flow rate ratio for the deposition, followed by a 2 minute Ar purge. The samples were then cleaved into 10 x 10 mm samples for the rapid thermal anneal (RTA) study. This consisted of four different temperatures (800, 850, 900 and 950°C) with 3 different annealing times (2, 15 and 30 minutes). The annealing was conducted in N_2 atmosphere (2000 sccm) in a JipElec RTA furnace. This procedure is illustrated in Figure 2.

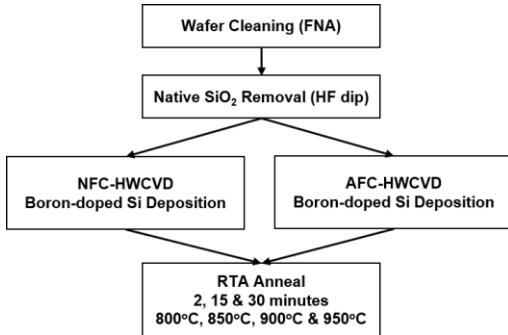


Figure 2: Process schematic of p-doped silicon film deposition and RTA.

Characterisation

Raman spectroscopy was used to characterise the crystallinity of both the as-deposited films as well as the annealed film samples. This was done using a Renishaw inVia confocal Raman microscope with a 532 nm laser. The Raman peaks of interest were analysed by defining each peak as a Voigt profile, which is the convolution of a Gaussian profile and Lorentzian profile. Using this method, we were able to identify the individual peaks that convoluted as a broad peak in our Raman spectra results.

In addition, the morphological irregularities of the top surface of the boron-doped emitter films were measured using a Veeco Metrology Multimode atomic force microscope (AFM) in tapping mode.

Results

Figure 3 shows the Stokes Raman peaks (between 400 – 600 cm^{-1}) for the as-deposited films for both the NFC and AFC conditions. From literature, we expect to see a peak at 520 cm^{-1} for crystalline silicon (c-Si), 512 cm^{-1} for micro-crystalline (μ c-Si) and 480 cm^{-1} for amorphous silicon (a-Si) [9, 10]. Both the NFC and AFC as-deposited films display a broad peak which extends across the 480 – 520 cm^{-1} Raman shift range. The shoulder-like peak present at 512 cm^{-1} is evidence that both of these films are micro-crystalline, with the sharp c-Si peak originating from the underlying substrate. Nonetheless, the relative area underneath the μ c-Si shoulder for AFC is smaller than the NFC film, suggesting that the increase in deposition temperature has led to a reduction in the μ c-Si content of the film and hence some epitaxial growth.

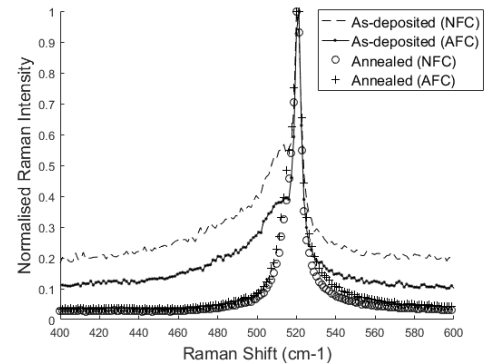


Figure 3: Normalised Raman spectra of both as-deposited films (unannealed) and 800°C anneal for 2 minutes of NFC and AFC deposited films.

Figure 3 also shows that after annealing both films for 2 minutes at 800°C, the μ c-Si shoulders have disappeared and only a sharp peak at 520 cm^{-1} is present, indicating that both films have crystallised. This was also the case for longer anneal times of 15 minutes and 30 minutes. This suggests that we can achieve a crystalline emitter from our HWCVD-deposited film with reduced annealing time and temperatures than previously reported.

Thermal stress effects from annealing at higher temperatures (beyond 800°C) on both the film quality and underlying substrate were also examined. As the

same trend was evident for both the NFC and AFC films, Figure 4 only shows the Raman spectra for the NFC films after being annealed for 2 minutes at temperatures from 800°C to 950°C. In addition, Table 1 displays the full-width at half maximum (FWHM) and position of the Raman peaks for the annealed films in Figure 4. It is important to note that based on the Voigt profile peak fitting method, the films annealed at 900°C and 950°C produced a secondary (μ c-Si) peak which was not apparent for the 800°C and 850°C annealed films. Therefore, in Table 1, the peak position and FWHM of only one (c-Si) peak is shown for the films annealed at 800°C and 850°C.

As seen in Figure 4 and the FWHM and peak positions in Table 1, the Raman peak for the annealed film broadens with higher anneal temperatures. Furthermore, when annealed at 900°C and 950°C, a secondary peak, in addition to the c-Si peak, appears at around 512 cm⁻¹. The FWHM also increases for the μ c-Si peak from 900°C to 950°C, despite the position of the peak remaining relatively constant. This suggests that increasing the annealing temperature is detrimental to the crystallinity of the film.

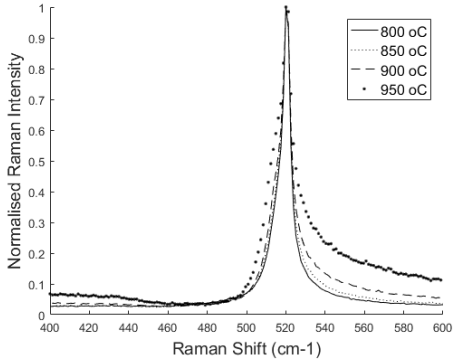


Figure 4: Normalised Raman spectra of the NFC deposited silicon film after 2 minutes RTA at 800 °C to 950 °C.

°C	c-Si peak		μ c-Si peak	
	FWHM	Position (cm ⁻¹)	FWHM	Position (cm ⁻¹)
800	2	519.8		
850	2	520.2		
900	0.3	520.2	6.9	512.3
950	0.4	520.8	7.9	512.4

Table 1: FWHM and peak position (cm⁻¹) of Raman peaks in Figure 4.

If the silicon film is highly doped (doping concentration $> 10^{18}$ cm⁻³), a resonant

interaction between the discrete optical phonon states and the continuum of energy levels in the valence and conduction band can occur [9, 11]. This Fano-type resonant interaction between phonon Raman scattering and electron Raman scattering is due to electron-phonon coupling and can induce a Fano-type silicon Raman peak asymmetry. This can be seen as a tail on the left side (for n-type doping) or right side (p-type doping) of the Raman peak. In Figure 4, an asymmetric tail is clearly demonstrated progressively with larger anneal temperatures, mainly on the right side of the peak. This is due to boron dopants being driven deeper into the n-type substrate from our deposited film, further signifying the detrimental effects of annealing at high temperatures.

In order to understand the morphology of these films further, AFM was used to scan the top surface of the as-deposited and annealed (2 minutes, 800°C) NFC film. A 3D-formatted scan across a 2 μ m x 2 μ m area of the as-deposited and annealed film is shown in Figure 5(a) and (b) respectively.

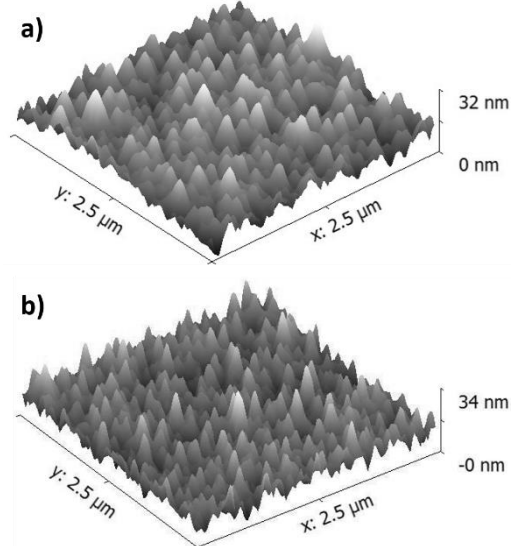


Figure 5: AFM image of (a) as-deposited NFC film and (b) after 2 minutes RTA at 800 °C.

The average surface roughness (RMS), R_a , was 3.9 nm and 4.1 nm for the as-deposited and annealed NFC film respectively, demonstrating a similarity between the morphology of these surfaces. Encouragingly, this roughness is lower than that presented by Rahman et al., despite higher temperature and longer anneal times [8]. However, the similarity in roughness and grain size between the as-deposited and annealed films would

suggest there is little change in surface morphology despite the Raman study shown in Figure 3 showing significantly improved crystallinity. This would suggest that during the annealing process, crystallisation, which starts from the interface with the substrate, has not fully proceeded to the surface. This would explain the discrepancy between the Raman measurement, which considers the bulk of the film, and AFM which is focused only on the surface. However, further studies need to be undertaken through AFM as well as scanning/transmission electron microscopy of longer annealed samples.

Conclusion

In this work, higher temperature deposition of doped silicon films using an altered filament configuration is shown to enhance crystallinity. However, a post-annealing step is still required to fully crystallise the film. A shortened annealing duration and temperature using an RTA process is investigated, with direct implications of the detrimental effects from using larger annealing temperatures on the film and junction quality being discussed. Based on Raman spectroscopy measurements of the deposited films, crystallisation is shown to be possible using a relatively short and low temperature post-anneal (2 minutes at 800°C). AFM data show that further fine-tuning is required to improve the surface.

In future work, we plan to characterise the temperatures in this tool based on different filament configurations, as well as analyse the electrical implications of these emitters for IBC silicon solar cells design.

References

- [1] K. Yoshikawa et al., "Silicon heterojunction solar cell with interdigitated back contacts for a photoconversion efficiency over 26%," *Nat. Energy*, vol. 2, 2017.
- [2] E. Franklin et al., "Design, fabrication and characterisation of a 24.4 % efficient interdigitated back contact solar cell," *Prog. Photovoltaics Res. Appl.*, vol. 15, pp. 659-676, 2014.
- [3] A. Ingenito et al., "Simplified process for high efficiency self aligned IBC c-Si solar cells combining ion implantation and epitaxial growth: Design and fabrication," *Sol. Energy Materials*, vol. 157, pp. 354-365, 2016.
- [4] T. Rahman et al., "Minimising bulk lifetime degradation during the processing of interdigitated back contact silicon solar cells," *Prog. Photovoltaics Res. Appl.*, vol. 26, no. 1, pp. 38-47, 2018.
- [5] T. Rahman et al., "Characterisation of epitaxial heavily-doped silicon regions formed by HWCVD using Micro-Raman and Micro-Photoluminescence Spectroscopy," *IEEE J. Photovoltaics*, In Press, 2018.
- [6] M. R. Payo et al., "Boron-doped selective silicon epitaxy: high efficiency and process simplification in interdigitated back contact cells," *Prog. Photovoltaic Res. Appl.*, vol. 15, pp. 711-725, 2013.
- [7] H. M. Branz et al., "Hot-wire chemical vapor deposition of epitaxial film crystal silicon for photovoltaics," *Thin Solid Films*, vol. 519, no. 14, pp. 4545-4550, 2011.
- [8] T. Rahman et al., "Junction formation with HWCVD and TCAD model of an epitaxial back-contact solar cell" *IEEE J. Photovoltaics*, vol. 6, pp. 1396-1402, 2016.
- [9] G. Sarau et al., "From Micro-to Macro-Raman Spectroscopy: Solar Silicon for a Case Study," *Adv. Asp. Spectrosc.*, pp. 221-246, 2012.
- [10] T. Kaneko et al., "Crystalline Fraction of Microcrystalline Silicon Films Prepared by Plasma-Enhanced Chemical Vapor Deposition Using Pulsed Silane Flow," *Jpn. J. Appl. Phys.*, vol. 32, pp. 4907-4911, 1993.
- [11] M. Becker et al., "Highly p-doped regions in silicon solar cells quantitatively analyzed by small angle bevelling and micro-Raman spectroscopy," *J. Appl. Phys.*, vol. 106, no. 7, 2009.